

New $N_f = 2$ Pseudofermion Action for Monte-Carlo Simulation of Lattice Field Theory with Domain-Wall Fermions

Yu-Chih Chen and Ting-Wai Chiu^{1,2,3}

¹ *Physics Department, National Taiwan Normal University, Taipei, Taiwan 11677, R.O.C.*

² *Institute of Physics, Academia Sinica, Taipei, Taiwan 11529, R.O.C.*

³ *Physics Department, National Taiwan University, Taipei, Taiwan 10617, R.O.C.*

Abstract

We construct a novel $N_f = 2$ pseudofermion action for Monte-Carlo simulation of lattice gauge theory with domain-wall fermions (DWF), of which the effective four-dimensional lattice Dirac operator is equal to the overlap-Dirac operator with the argument of the sign function equal to $H = c\gamma_5 D_w(1 + dD_w)^{-1}$, where c and d are parameters, and D_w is the standard Wilson-Dirac operator plus a negative parameter $-m_0$ ($0 < m_0 < 2$). This new action is particularly useful for the challenging simulations of lattice gauge theories with large $N_f = 2n$ DWF, on the large lattices, and in the strong-coupling regime.

I. INTRODUCTION

In lattice gauge theory with N_f dynamical domain-wall fermions (DWF) [1], one often considers the cases containing two fermions with degenerate masses. For example, $N_f = 2$, $N_f = 2 + 1$, and $N_f = 2 + 1 + 1$ QCD, in which the masses of **u** and **d** quarks are degenerate, i.e., the theory in the isospin symmetry limit. For hybrid Monte-Carlo (HMC) simulations [2] of these theories, we have been using the $N_f = 2$ pseudofermion action as given in Ref. [3]. Recently, for studies relating to the beyond Standard Model with composite Higgs boson, one investigates whether a lattice gauge theory with a large number of massless fermions can possess an infrared conformal fixed-point, e.g., the $SU(3)$ lattice gauge theory with $N_f = 10$ massless fermions, in which the pseudofermion action can be written as the sum of five identical $N_f = 2$ massless pseudofermion actions. However, the HMC simulation based on the traditional $N_f = 2$ pseudofermion action turns out to be rather time-consuming for large lattices at strong couplings. In this paper, we construct a new $N_f = 2$ pseudofermion action for all variants of DWF, which is more efficient than the traditional $N_f = 2$ pseudofermion action for the HMC simulation of the theories with large $N_f = 2n$ massless DWF, especially for large lattices in the strong-coupling regime, as first reported in Ref. [4]. In this paper, we demonstrate that, for the $SU(3)$ lattice gauge theory with $N_f = 10$ massless Möbius DWF on the 32^4 lattice at $6/g_0^2 = 5.70$, the efficiency (speed \times acceptance rate) of the HMC simulation with the new action is about 1.2 times of its counterpart with the traditional action.

In general, the 5-dimensional lattice Dirac operator of any kind of DWF with infinite extent in the fifth dimension ($N_s = \infty$) gives the effective 4-dimensional lattice Dirac operator equal to

$$D(m_q) = m_q + \frac{1}{2r}(1 - rm_q) \left[1 + \gamma_5 \frac{H}{\sqrt{H^2}} \right], \quad (1)$$

where m_q is the bare quark mass,

$$H = c\gamma_5 D_w (1 + dD_w)^{-1}, \quad (2)$$

$$r = \frac{1}{2m_0(1 - dm_0)}, \quad (3)$$

and D_w is the standard Wilson Dirac operator plus a negative parameter $-m_0$ ($0 < m_0 < 2$). Here c and d are parameters to specify the type of DWF. Setting $m_q = 0$, $c = 1$ and $d = 0$,

(1) becomes the massless overlap-Dirac operator [5, 6],

$$D_{ov} = m_0 \left[1 + D_w (D_w^\dagger D_w)^{-1/2} \right] = m_0 \left[1 + \gamma_5 \frac{H_w}{\sqrt{H_w^2}} \right], \quad H_w = \gamma_5 D_w.$$

In other words, the effective 4-dimensional lattice Dirac operator (1) of any kind of DWF can be regarded as the generalized overlap-Dirac operator with the argument of the sign function equal to H (2). In the massless limit $m_q = 0$, (1) satisfies the Ginsparg-Wilson relation [7]

$$D\gamma_5 + \gamma_5 D = 2rD\gamma_5 D \iff D^{-1}\gamma_5 + \gamma_5 D^{-1} = 2r\gamma_5 \mathbb{I},$$

where the chiral symmetry is broken by a contact term, i.e., the exact chiral symmetry at finite lattice spacing.

On the 5-dimensional lattice with size $(N_x^3 \times N_t \times N_s)$, the lattice fermion operator of all variants of DWF [8–11] can be written as

$$[\mathcal{D}(m_q)]_{xx';ss'} = (\rho_s D_w + 1)_{xx'} \delta_{ss'} + (\sigma_s D_w - 1)_{xx'} L_{ss'}, \quad (4)$$

where s and s' are the indices in the fifth dimension, x and x' denote the lattice sites on the 4-dimensional lattice, and the Dirac and color indices have been suppressed. Here D_w is the standard Wilson Dirac operator plus a negative parameter $-m_0$ ($0 < m_0 < 2$),

$$(D_w)_{xx'} = (4 - m_0) - \frac{1}{2} \sum_{\hat{\mu}=1}^4 [(1 - \gamma_\mu) U_\mu(x) \delta_{x+\hat{\mu},x'} + (1 + \gamma_\mu) U_\mu^\dagger(x') \delta_{x-\hat{\mu},x'}],$$

where $U_\mu(x)$ denotes the link variable pointing from x to $x+\hat{\mu}$. The operator L is independent of the gauge field, and it can be written as

$$L = P_+ L_+ + P_- L_-, \quad P_\pm = (1 \pm \gamma_5)/2, \quad (5)$$

where

$$(L_+)_{ss'} = \begin{cases} -rm_q \delta_{N_s, s'}, & s = 1, \\ \delta_{s-1, s'}, & 1 < s \leq N_s \end{cases}, \quad L_- = (L_+)^T. \quad (6)$$

Note that the matrices L_\pm satisfy $L_\pm^T = L_\mp$, and $R_5 L_\pm R_5 = L_\mp$, where R_5 is the reflection operator in the fifth dimension, with elements $(R_5)_{ss'} = \delta_{s', N_s+1-s}$. Thus $R_5 L_\pm$ is real and symmetric.

For all variants of DWF in Refs. [8–11], we write $\rho_s = c\omega_s + d$, and $\sigma_s = c\omega_s - d$, where c , d , and $\{\omega_s\}$ are parameters to specify the type of DWF. For the conventional DWF with the Shamir kernel [8], $c = d = 1/2$, and $\omega_s = 1, \forall s$. For the Borici DWF [9], $c = 1$, $d = 0$, and $\omega_s = 1, \forall s$. For the optimal DWF [10], the weights $\{\omega_s\}$ are fixed according to the formula derived in [10] such that the maximal chiral symmetry is attained, i.e., its effective 4-dimensional Dirac operator is exactly equal to the Zolotarev optimal rational approximation of (1). For the Möbius DWF [11], $\omega_s = 1, \forall s$.

Using the lattice DWF operator (4), and including the Pauli-Villars fields with bare mass $m_{PV} = 1/r = 2m_0(1 - dm_0)$, the pseudofermion action for all variants of DWF can be written as

$$S = \phi^\dagger \frac{\mathcal{D}(m_{PV})}{\mathcal{D}(m_q)} \phi, \quad (7)$$

where ϕ and ϕ^\dagger are complex scalar fields carrying the same quantum numbers (color, spin) of the fermion fields. Integrating the pseudofermion fields in the fermionic partition function gives the fermion determinant of the effective 4-dimensional lattice Dirac operator at finite N_s

$$\int [d\phi^\dagger][d\phi] \exp \left\{ -\phi^\dagger \frac{\mathcal{D}(m_{PV})}{\mathcal{D}(m_q)} \phi \right\} = \det \frac{\mathcal{D}(m_q)}{\mathcal{D}(m_{PV})} = \det D_{N_s}(m_q),$$

where

$$D_{N_s}(m_q) = m_q + \frac{1}{2r}(1 - rm_q)[1 + \gamma_5 S_{N_s}(H)],$$

$$S_{N_s}(H) = \frac{1 - \prod_{s=1}^{N_s} T_s}{1 + \prod_{s=1}^{N_s} T_s}, \quad T_s = \frac{1 - \omega_s H}{1 + \omega_s H}.$$

In the limit $N_s \rightarrow \infty$, $S_{N_s}(H) \rightarrow H/\sqrt{H^2}$, thus $D_{N_s}(m_q) \rightarrow D(m_q)$ in (1). For finite N_s , if the weights $\{\omega_s, s = 1, \dots, N_s\}$ are fixed according to the formulas derived in Ref. [10], $S_{N_s}(H)$ is equal to the Zolotarev optimal rational approximation of $H/\sqrt{H^2}$. On the other hand, if the weights $\omega_s = 1, \forall s$, $S_{N_s}(H)$ is equal to the polar approximation of $H/\sqrt{H^2}$.

Note that the pseudofermion action (7) for $N_f = 1$ DWF cannot be used for HMC simulations, since $\mathcal{D}(m_{PV})\mathcal{D}^{-1}(m_q)$ is not positive-definite and Hermitian. A positive-definite, Hermitian, and exact pseudofermion action for $N_f = 1$ DWF has been constructed in Ref. [12]. For $N_f = 2$, it is straightforward to construct a positive-definite and Hermitian pseudofermion action from (7),

$$S^{N_f=2} = \phi^\dagger \mathcal{D}^\dagger(m_{PV})[\mathcal{D}(m_q)\mathcal{D}^\dagger(m_q)]^{-1}\mathcal{D}(m_{PV})\phi.$$

However, this $N_f = 2$ pseudofermion action is not efficient for the HMC simulation.

The outline of this paper is as follows. In section 2, we derive the traditional $N_f = 2$ pseudofermion action for DWF, which we have been using for the simulations of $N_f = 2$ and $N_f = 2+1+1$ lattice QCD. Even though the derivation of this $N_f = 2$ pseudofermion action has been given in Ref. [13], we present a different derivation here, mainly for defining our notations in this paper. In section 3, we construct the new $N_f = 2$ pseudofermion action for all variants of DWF. In section 4, we perform numerical simulations to compare the HMC efficiencies of the new and the old actions. In section 5, we conclude with some remarks.

II. THE TRADITIONAL $N_f = 2$ PSEUDOFERMION ACTION

Using $\rho_s = c\omega_s + d$, and $\sigma_s = c\omega_s - d$, (4) can be rewritten as

$$\mathcal{D}(m_q) = D_w[c\omega(1+L) + d(1-L)] + 1 - L,$$

where L is defined in (5) and (6). Since $\det[\mathcal{D}(m_q)] = \det[\omega^{-1/2}\mathcal{D}(m_q)\omega^{1/2}]$, we can use $\omega^{-1/2}\mathcal{D}(m_q)\omega^{1/2}$ for the HMC simulation. Moreover, L and $\omega = \text{diag}(\omega_1, \dots, \omega_{N_s})$ are independent of the gauge field, we can drop the factor $[c\omega^{1/2}(1+L)\omega^{1/2} + d\omega^{-1/2}(1-L)\omega^{1/2}]$ from $\omega^{-1/2}\mathcal{D}(m_q)\omega^{1/2}$, and obtain the re-scaled DWF operator for HMC,

$$D_T(m_q) = D_w + \omega^{-1/2} \{c[1+L(m_q)][1-L(m_q)]^{-1} + d\omega^{-1}\}^{-1} \omega^{-1/2} = D_w + M(m_q), \quad (8)$$

where

$$M(m_q) = P_+M_+(m_q) + P_-M_-(m_q), \quad P_{\pm} = (1 \pm \gamma_5)/2, \quad (9)$$

$$M_{\pm}(m_q) = \omega^{-1/2} \{cN_{\pm}(m_q) + d\omega^{-1}\}^{-1} \omega^{-1/2}, \quad (10)$$

$$N_{\pm}(m_q) = [1 + L_{\pm}(m_q)][1 - L_{\pm}(m_q)]^{-1}. \quad (11)$$

Here the dependence on m_q has been shown explicitly in L_{\pm} , M_{\pm} , and N_{\pm} .

Next, we perform the even-odd preconditioning on $D_T(m_q)$. This is essential for halving the memory footprint as well as lowering the condition number of the conjugate gradient solver for the fermion force. With even-odd preconditioning on the 4-dimensional space-time lattice, (8) can be written as

$$D_T(m_q) = \begin{pmatrix} M_5^{-1}(m_q) & D_w^{\text{EO}} \\ D_w^{\text{OE}} & M_5^{-1}(m_q) \end{pmatrix} \quad (12)$$

where

$$M_5^{-1}(m_q) = 4 - m_0 + M(m_q). \quad (13)$$

Using the Schur decomposition, (12) becomes

$$D_T(m_q) = \begin{pmatrix} 1 & 0 \\ D_w^{\text{OE}} M_5 & 1 \end{pmatrix} \begin{pmatrix} M_5^{-1} & 0 \\ 0 & M_5^{-1} C \end{pmatrix} \begin{pmatrix} 1 & M_5 D_w^{\text{EO}} \\ 0 & 1 \end{pmatrix} \quad (14)$$

where

$$C(m_q) \equiv 1 - M_5(m_q) D_w^{\text{OE}} M_5(m_q) D_w^{\text{EO}}. \quad (15)$$

Since $\det D_T = \det M_5^{-2} \cdot \det C$, and M_5 does not depend on the gauge field, we can just use C in the Monte Carlo simulation. After including the Pauli-Villars fields with mass $m_{PV} = 2m_0(1 - dm_0)$, we obtain the $N_f = 2$ pseudofermion action for all variants of DWF,

$$S = \phi^\dagger C^\dagger(m_{PV}) \{C(m_q) C^\dagger(m_q)\}^{-1} C(m_{PV}) \phi, \quad (16)$$

which has been used for the HMC simulations of $N_f = 2$, and $N_f = 2 + 1 + 1$ lattice QCD with the optimal DWF [14–16].

III. THE NEW $N_f = 2$ PSEUDOFERMION ACTION

From (8), it gives the ratio

$$\begin{aligned} \frac{\det[D_T(m_{PV})]}{\det[D_T(m_q)]} &= \frac{\det[D_w + M(m_{PV})]}{\det[D_w + M(m_q)]} \\ &= \frac{\det[H_T(m_q) + \gamma_5 \Delta(m_q)]}{\det[H_T(m_q)]} = \det \left[1 + \gamma_5 \Delta(m_q) \frac{1}{H_T(m_q)} \right], \end{aligned} \quad (17)$$

where $\det R_5$ and $\det \gamma_5$ have been multiplied in both the numerator and the denominator, and

$$\begin{aligned} H_T(m_q) &= R_5 \gamma_5 D_T(m_q), \\ \Delta(m_q) &= R_5 [M(m_{PV}) - M(m_q)] = P_+ \Delta_+(m_q) + P_- \Delta_-(m_q). \end{aligned}$$

Following Ref. [12], $\Delta_\pm(m_q)$ can be simplified as follows. From (11), it gives the relation

$$N_\pm(m_q) = N_\pm(0) - \frac{2rm_q}{1 + rm_q} uu^T, \quad u^T \equiv (1, 1, \dots, 1).$$

Then using the Sherman-Morrison formula, we obtain

$$[cN_{\pm}(m_q) + d\omega^{-1}]^{-1} = A_{\pm}^{-1} + \frac{2crm_q}{1 + rm_q - 2crm_q\lambda_{\pm}} A_{\pm}^{-1} u u^T A_{\pm}^{-1}, \quad (18)$$

where

$$\begin{aligned} A_{\pm} &= cN_{\pm}(0) + d\omega^{-1}, \\ \lambda_{\pm} &= u^T A_{\pm}^{-1} u. \end{aligned}$$

Now using the optimal ω which is invariant under R_5 (i.e., $R_5\omega R_5 = \omega$) [17], defining $v_{\pm} \equiv R_5 A_{\pm}^{-1} u$, and putting (18) into (10), we obtain

$$M_{\pm}(m_q) = \omega^{-1/2} A_{\pm}^{-1} \omega^{-1/2} + \frac{2crm_q}{1 + rm_q - 2crm_q\lambda_{\pm}} R_5 \omega^{-1/2} v_{\pm} v_{\pm}^T \omega^{-1/2}, \quad (19)$$

where we have used

$$u^T A_{\pm}^{-1} = u^T R_5 R_5 A_{\pm}^{-1} R_5 R_5 = u^T (A_{\pm}^{-1})^T R_5 = (R_5 A_{\pm}^{-1} u)^T = v_{\pm}^T.$$

Since A_{\pm}^{-1} is an lower/upper triangular matrix, we can solve for v_{\pm} (vectors in the fifth dimensional space) with the following recursion relation,

$$\begin{aligned} (v_+)_{N_s} &= (v_-)_1 = \alpha_{N_s}, \\ (v_+)_{s} &= (v_-)_{N_s-s+1} = \alpha_s \beta_{s+1} (v_+)_{s+1}, \quad s = N_s - 1, \dots, 1, \end{aligned}$$

where $\alpha_s = 1/(c + d\omega_s^{-1})$ and $\beta_s = -c + d\omega_s^{-1}$. Then we obtain

$$\lambda_- = \lambda_+ = u^T A_{+}^{-1} u = u^T R_5 A_{+}^{-1} u = u^T v_+ = \sum_s (v_+)_{s} = \sum_s \alpha_s Q_s \equiv \lambda,$$

where $Q_s \equiv \alpha_{s+1} \beta_{s+1} \dots \alpha_{N_s} \beta_{N_s}$. Using (19), we obtain

$$\Delta_{\pm}(m_q) = R_5 [M_{\pm}(m_{PV}) - M_{\pm}(m_q)] = k\omega^{-1/2} v_{\pm} v_{\pm}^T \omega^{-1/2}, \quad (20)$$

where

$$k = \frac{c}{1 - c\lambda} \left(\frac{1 - rm_q}{1 + rm_q - 2crm_q\lambda} \right), \quad r = \frac{1}{2m_0(1 - dm_0)}.$$

Putting (20) into (17) and using the identity $\det(1 + AB) = \det(1 + BA)$, (17) becomes

$$\frac{\det[D_T(m_{PV})]}{\det[D_T(m_q)]} = \det \left[1 + k\gamma_5 v^T \omega^{-1/2} \frac{1}{H_T(m_q)} \omega^{-1/2} v \right] = \det K(m_q)$$

where

$$K(m_q) = 1 + k\gamma_5 v^T \omega^{-1/2} \frac{1}{H_T(m_q)} \omega^{-1/2} v, \quad v = P_+ v_+ + P_- v_-. \quad (21)$$

Note that $K(m_q)$ is an operator on the 4-dimensional space, similar to the positive-definite Hermitian operators H_1 and H_2 in the exact pseudofermion action for one-flavor DWF [12]. However, $K(m_q)$ is not Hermitian. For the $N_f = 2$ pseudofermion action, it can be constructed as

$$S_{\text{new}} = \phi^\dagger K^\dagger(m_q) K(m_q) \phi, \quad (22)$$

where ϕ and ϕ^\dagger are pseudofermion fields on the 4-dimensional lattice. This is the main result of this paper.

IV. NUMERICAL RESULTS

To compare the efficiencies and characteristics of the HMC simulations with the new action and the traditional action, we focus on the challenging simulations of lattice gauge theories with large $N_f = 2n$ massless DWF on a large lattice. Here we perform HMC simulations of the $SU(3)$ lattice gauge theory with $N_f = 10$ massless fermions on the 32^4 lattice, using the Möbius DWF ($c = 1$, $d = 1/2$ and $\omega_s = 1, \forall s$) with $N_s = 16$ and $m_0 = 1.8$, and the Wilson plaquette gauge action at $6/g_0^2 = 5.70$. Since to simulate $N_f = 10$ fermions amounts to simulate 5 pairs of $N_f = 2$ fermions, for the traditional $N_f = 2$ pseudofermion action (16), the partition function of the $SU(3)$ gauge theory with $N_f = 10$ massless DWF can be written as

$$Z = \int [dU] \prod_{i=1}^5 [d\phi_i^\dagger][d\phi_i] \exp \left(-S_g[U] - \sum_{i=1}^5 \phi_i^\dagger C_i^\dagger(m_{PV}) [C_i(0)C_i^\dagger(0)]^{-1} C_i(m_{PV}) \phi_i \right), \quad (23)$$

where ϕ_i and ϕ_i^\dagger are pseudofermion fields, $m_{PV} = m_0(2 - m_0) = 0.36$ is the mass of the Pauli-Villars fields, and $S_g(U)$ is the Wilson plaquette gauge action

$$S_g(U) = \frac{6}{g_0^2} \sum_{\text{plaq.}} \left\{ 1 - \frac{1}{3} \text{ReTr}(U_p) \right\}.$$

Similarly, using the new $N_f = 2$ pseudofermion action (22), the partition function of the $SU(3)$ lattice gauge theory with $N_f = 10$ massless fermions can be written as

$$Z_{\text{new}} = \int [dU] \prod_{i=1}^5 [d\phi_i^\dagger][d\phi_i] \exp \left(-S_g[U] - \sum_{i=1}^5 \phi_i^\dagger K(0)^\dagger K(0) \phi_i \right). \quad (24)$$

In both cases, the boundary conditions of the gauge field are periodic in all directions, while the boundary conditions of the pseudofermion fields are antiperiodic in all directions. In the molecular dynamics, we use the Omelyan integrator [18], and the Sexton-Weingarten multiple-time scale method [19]. Moreover, we introduce auxiliary heavy fermion fields (with mass $m_H a = 0.1$) for the mass-preconditioning, similar to the case of Wilson fermion [20]. Each simulation is performed on a single Nvidia GTX-TITAN. The thermalization for the HMC simulation with the traditional/new action takes 164/172 trajectories, then to generate 78/79 trajectories after thermalization. The total computation time for the case with the traditional action takes about 58 days, while that with the new action about 50 days. The HMC characteristics based on the thermalized trajectories are summarized in Table I.

TABLE I: Summary of the HMC characteristics for the $SU(3)$ gauge theory with $N_f = 10$ massless DWF.

	Time(s)/traj	Acceptance	$\langle \Delta H \rangle$	$P_{\text{acc}} = \text{erfc}(\sqrt{\langle \Delta H \rangle}/2)$	$\langle \exp(-\Delta H) \rangle$	$\langle \text{plaquette} \rangle$
Traditional	20455(40)	0.846(41)	0.053(34)	0.871(44)	1.011(35)	0.57381(2)
New	16992(36)	0.823(43)	0.110(47)	0.814(40)	0.983(54)	0.57384(2)

In Fig. 1, we plot the computational time for each HMC trajectory in the HMC simulations of the $SU(3)$ lattice gauge theory with $N_f = 10$ massless Möbius DWF. From the first column of Table I, the average speed of the simulation with the new action is more than 1.2 times of its counterpart with the traditional action. Moreover, from the second column of Table I, the acceptance rate with the new action is 0.823(43), compatible with its counterpart with the traditional action, 0.846(41). Taking into account of both the speed and the acceptance rate, the HMC efficiency (speed \times acceptance rate) with the new action is estimated to be about 1.2 times of its counterpart with the traditional action. In the following, we present more details of the simulations.

In Fig. 2, we plot the maximum force (averaged over all links) among all momentum updates in each trajectory, for the gauge field, the heavy fermion field, and the light fermion field respectively. Here only the fermion forces corresponding to the first pair of pseudofermions are plotted, i.e., for $i = 1$ in (23) and (24). The fermion forces for $i = 2, \dots, 5$ behave similar to those of $i = 1$, thus are omitted. For both (a) and (b), the forces all behave smoothly for all trajectories. However, the fermion forces in (b) with the new action

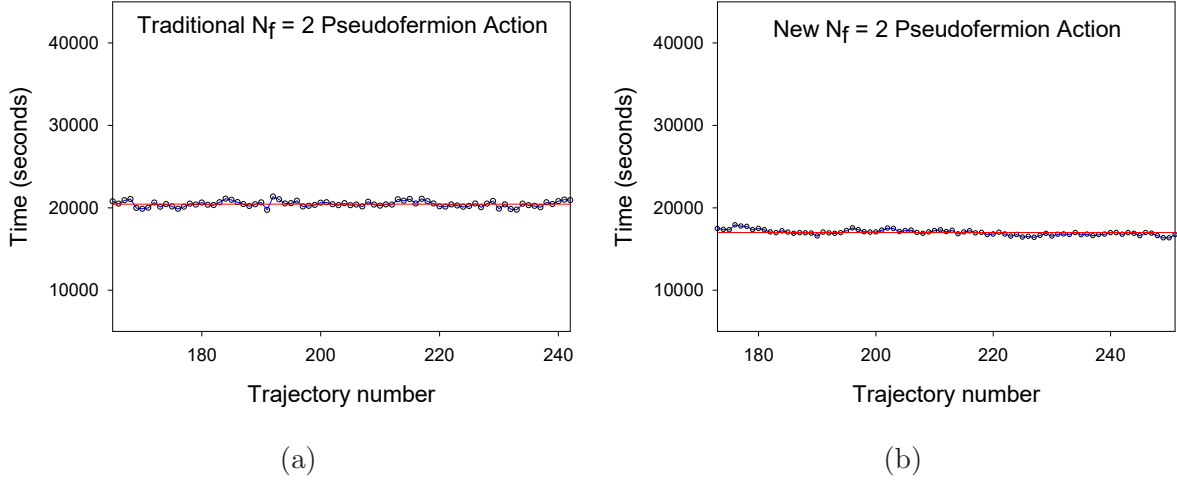


FIG. 1: The computational time for each trajectory in the HMC simulation of the $SU(3)$ lattice gauge theory with $N_f = 10$ massless Möbius DWF, (a) the traditional action, and (b) the new action. The horizontal line is the average computational time per trajectory. The line connecting the data points is only for guiding the eyes.

are substantially smaller than their counterparts in (a) with the traditional action. This immediately implies that the step sizes (in the Omelyan integrator) for the momentum update with the fermion forces in the case with the new action can be larger than their counterparts with the traditional action. With the length of the HMC trajectory equal to one, we use 3 different time scales for the momentum update with the gauge force, the heavy-fermion force, and the light-fermion force, which correspond to the step sizes $1/(k_0 k_1 k_2)$, $1/(k_1 k_2)$, and $1/k_2$ respectively. In our simulations, we set $(k_0, k_1, k_2) = (10, 2, 14)$ for the traditional action, while $(k_0, k_1, k_2) = (10, 2, 5)$ for the new action.

In Fig. 3, we plot the change of Hamiltonian ΔH versus the HMC trajectory after thermalization. For (a) with the traditional action, the fluctuation of ΔH is small, without large spikes in all trajectories. On the other hand, for (b) with the new action, the fluctuation of ΔH is slightly larger than that in (a) with the traditional action. Consequently, the acceptance rate of (b) with the new action is 0.823(43), slightly lower than that 0.846(41) of (a) with the traditional action, as summarized in Table I. By measuring the expectation value of ΔH , we can obtain the theoretical estimate of the acceptance rate for HMC, $P_{\text{acc}} = \text{erfc} \left(\sqrt{\langle \Delta \mathcal{H} \rangle} / 2 \right)$ [21], which can be compared with the measured acceptance rate. As shown in Table I, the measured acceptance rate is consistent with the theoretical acceptance rate

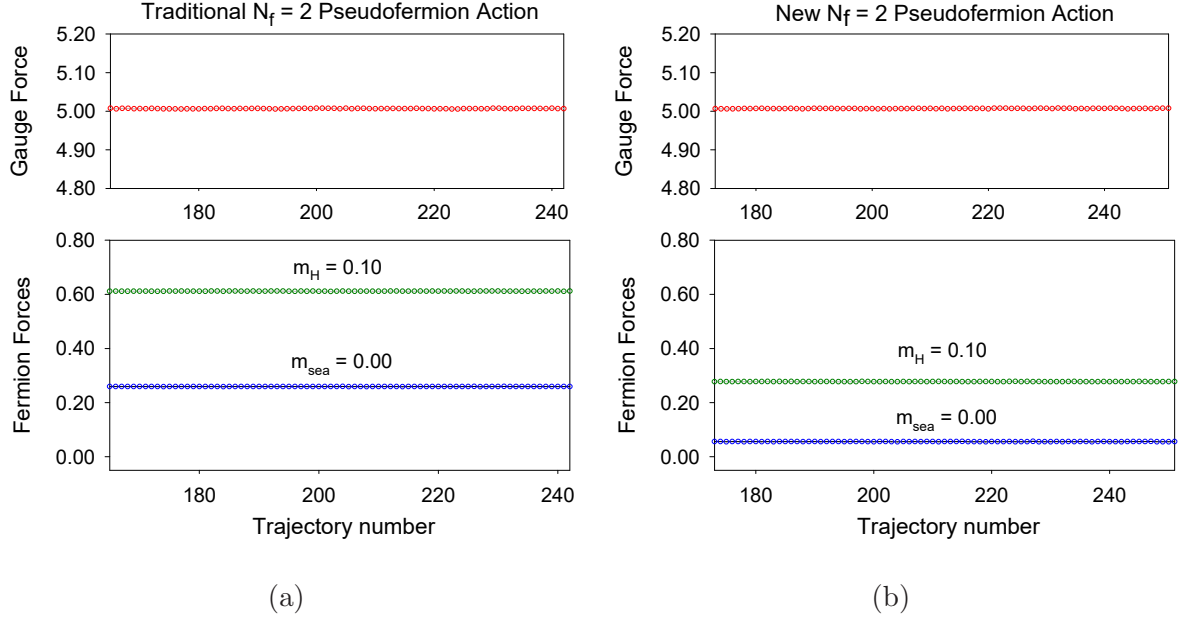


FIG. 2: The maximum forces of the gauge field, the heavy fermion field, and the light fermion field versus the HMC trajectory in the HMC simulations of the lattice gauge theory with $N_f = 10$ massless Möbius DWF, (a) the traditional action, and (b) the new action. Here only the fermion forces corresponding to the first pair of pseudofermions are plotted, i.e., for $i = 1$ in (23) and (24).

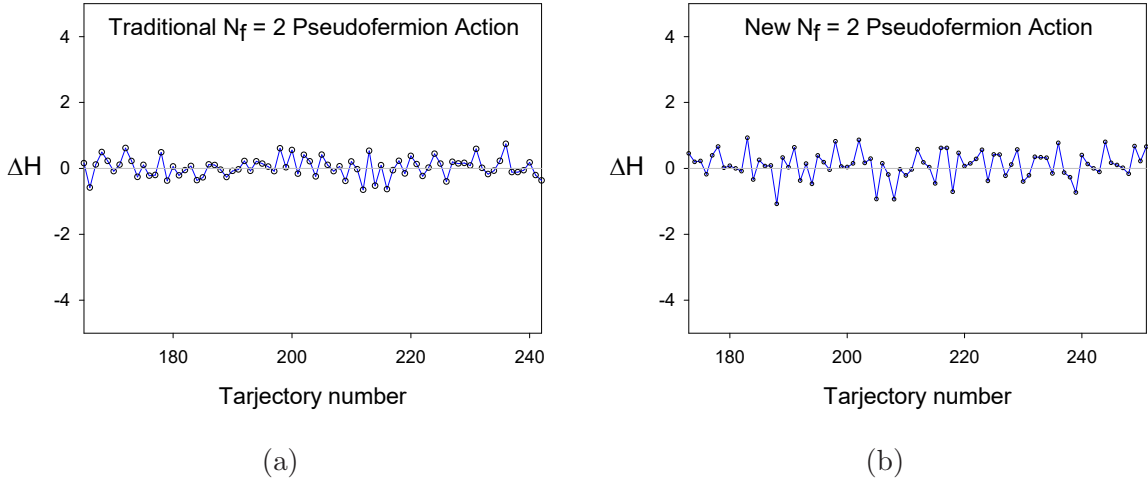


FIG. 3: The change of Hamiltonian ΔH versus the trajectory in the HMC simulations of the lattice gauge theory with $N_f = 10$ massless Möbius DWF, for (a) the traditional action, and (b) the new action. The line connecting the data points is only for guiding the eyes.

for both cases with the traditional and the new actions.

Next, we measure the expectation value of $\exp(-\Delta H)$, to check whether it is consistent with the theoretical formula $\langle \exp(-\Delta H) \rangle = 1$ which follows from the area-preserving property of the HMC simulation [22]. For both cases with the traditional and the new actions, the measured values are 1.011(35) and 0.983(54) respectively, in good agreement with the theoretical expectation value.

Finally, it is interesting to find out what is the renormalized coupling of this $SU(3)$ gauge theory with $N_f = 10$ massless Möbius DWF at $6/g_0^2 = 5.70$. Performing the Wilson flow [23, 24] with the small number (~ 80) of thermalized gauge configurations generated in this test, we obtain an estimate of the renormalized coupling $g_c^2(L, a) \sim 4.5$ in the finite-volume gradient flow scheme [25] with $c = \sqrt{8t}/L = 0.3$, which is much less than the largest coupling $g_c^2 \sim 7.0$ studied in Ref. [4].

V. CONCLUDING REMARK

To summarize, we have constructed a new $N_f = 2$ pseudofermion action for lattice gauge theory with DWF. Moreover, we demonstrate that for the $SU(3)$ gauge theory with $N_f = 10$ massless Möbius DWF, the efficiency (speed \times acceptance rate) of the HMC simulation with the new action is about 1.2 times of its counterpart with the traditional action. We expect that the gain of using the new $N_f = 2$ pseudofermion action would become higher for more challenging simulations, i.e., lattice gauge theories with larger $N_f = 2n$ (e.g., $N_f = 12$) massless DWF, on larger lattices (e.g., 64^4), and in the stronger coupling regime. Note that for the $SU(3)$ lattice gauge theory with $N_f = 10$ massless optimal DWF, one of us (TWC) encountered great difficulties (low acceptance rate and/or long simulation time) in the HMC simulation with the traditional $N_f = 2$ pseudofermion action, on the 32^4 lattice at $\beta = 6/g_0^2 = 6.45$ [26]. The difficulties were circumvented by switching to the new $N_f = 2$ pseudofermion action, and obtaining $g_c^2(L, a) \sim 8.6$ in the finite-volume gradient flow scheme with $c = \sqrt{8t}/L = 0.3$. Nevertheless, a detailed study to compare the HMC efficiencies and characteristics of this theory with the new and the traditional actions is beyond the scope of this paper, since a single GPU (e.g., Nvidia GTX-TITAN) would take more than one year to generate 200-300 trajectories in the HMC with the traditional $N_f = 2$ pseudofermion action.

In general, there is no guarantee that the new action would outperform the traditional

action for any lattice field theory. In practice, one needs to perform numerical experiments to find out which action has higher HMC efficiency for the theory in question, which also depends on the computational platform and the algorithm implementation. Most importantly, now we have a new pseudofermion action to tackle the challenging simulations of lattice gauge theories with large $N_f = 2n$ massless domain-wall fermions.

Acknowledgments

This work is supported by the Ministry of Science and Technology (Grant Nos. 108-2119-M-003-005, 107-2119-M-003-008, 105-2112-M-002-016, 102-2112-M-002-019-MY3), and the National Center for Theoretical Sciences (Physics Division). We gratefully acknowledge the computer resources provided by Academia Sinica Grid Computing Center (ASGC), and National Center for High Performance Computing (NCHC).

-
- [1] D. B. Kaplan, Phys. Lett. B **288**, 342 (1992) [hep-lat/9206013].
 - [2] S. Duane, A. D. Kennedy, B. J. Pendleton and D. Roweth, Phys. Lett. B **195**, 216 (1987).
 - [3] T. W. Chiu, T. H. Hsieh, Y. Y. Mao [TWQCD Collaboration], Phys. Lett. B **717**, 420 (2012) [arXiv:1109.3675 [hep-lat]].
 - [4] T. W. Chiu, Phys. Rev. D **99**, no. 1, 014507 (2019) [arXiv:1811.01729 [hep-lat]].
 - [5] H. Neuberger, Phys. Lett. B **417**, 141 (1998) [hep-lat/9707022].
 - [6] R. Narayanan and H. Neuberger, Nucl. Phys. B **443**, 305 (1995) [hep-th/9411108].
 - [7] P. H. Ginsparg and K. G. Wilson, Phys. Rev. D **25**, 2649 (1982).
 - [8] Y. Shamir, Nucl. Phys. B **406**, 90 (1993) [hep-lat/9303005].
 - [9] A. Borici, Nucl. Phys. Proc. Suppl. **83** (2000) 771 [hep-lat/9909057].
 - [10] T. W. Chiu, Phys. Rev. Lett. **90**, 071601 (2003) [hep-lat/0209153].
 - [11] R. C. Brower, H. Neff and K. Orginos, Nucl. Phys. Proc. Suppl. **140**, 686 (2005) [hep-lat/0409118].
 - [12] Y. C. Chen and T. W. Chiu [TWQCD Collaboration], Phys. Lett. B **738**, 55 (2014) [arXiv:1403.1683 [hep-lat]].
 - [13] T. W. Chiu [TWQCD Collaboration], J. Phys. Conf. Ser. **454**, 012044 (2013) [arXiv:1302.6918]

- [hep-lat]].
- [14] W. P. Chen, Y. C. Chen, T. W. Chiu, H. Y. Chou, T. S. Guu, T. H. Hsieh [TWQCD Collaboration], Phys. Lett. B **736**, 231 (2014) [arXiv:1404.3648 [hep-lat]].
 - [15] Y. C. Chen and T. W. Chiu [TWQCD Collaboration], Phys. Lett. B **767**, 193 (2017) [arXiv:1701.02581 [hep-lat]].
 - [16] T. W. Chiu [TWQCD Collaboration], PoS LATTICE **2018**, 040 (2018) [arXiv:1811.08095 [hep-lat]].
 - [17] T. W. Chiu, Phys. Lett. B **744**, 95 (2015) [arXiv:1503.01750 [hep-lat]].
 - [18] I.P. Omelyan, I.M. Mryglod, and R. Folk, Phys. Rev. Lett. **86**, 898 (2001).
 - [19] J. C. Sexton and D. H. Weingarten, Nucl. Phys. B **380**, 665 (1992).
 - [20] M. Hasenbusch, Phys. Lett. B **519**, 177 (2001) [hep-lat/0107019].
 - [21] S. Gupta, A. Irback, F. Karsch and B. Petersson, Phys. Lett. B **242**, 437 (1990).
 - [22] M. Creutz, Phys. Rev. D **38**, 1228 (1988).
 - [23] R. Narayanan and H. Neuberger, JHEP **0603**, 064 (2006) [hep-th/0601210].
 - [24] M. Luscher, JHEP **1008**, 071 (2010), Erratum: [JHEP **1403**, 092 (2014)] [arXiv:1006.4518 [hep-lat]].
 - [25] Z. Fodor, K. Holland, J. Kuti, D. Negradi and C. H. Wong, JHEP **1211**, 007 (2012) [arXiv:1208.1051 [hep-lat]].
 - [26] T. W. Chiu, PoS LATTICE **2016**, 228 (2017).